

X-ray fluorescence spectroscopy from ions at charged vapor/water interfaces

Wei Bu and David Vaknin

Citation: *J. Appl. Phys.* **105**, 084911 (2009); doi: 10.1063/1.3117487

View online: <http://dx.doi.org/10.1063/1.3117487>

View Table of Contents: <http://jap.aip.org/resource/1/JAPIAU/v105/i8>

Published by the American Institute of Physics.

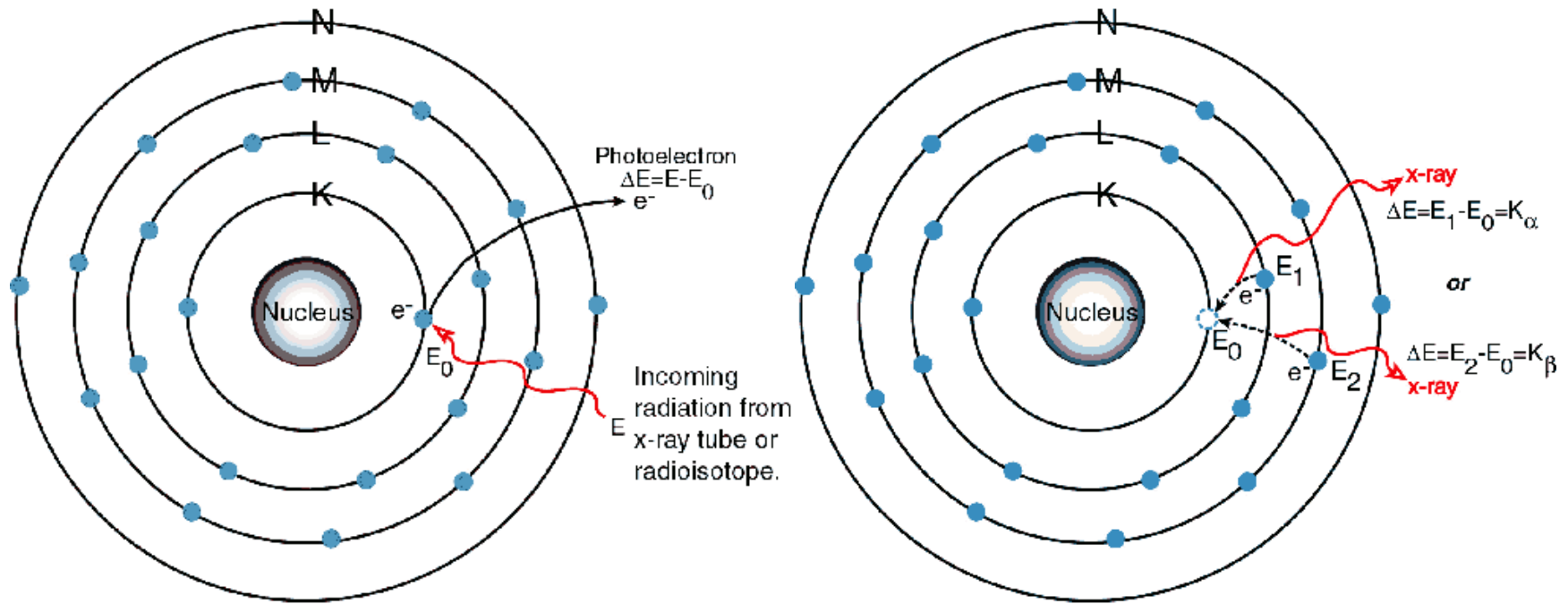
X-ray fluorescence spectra from monovalent ions (Cs^+) that accumulate from dilute solutions to form an ion-rich layer near a charged Langmuir monolayer are presented. For the salt solution without the monolayer, the fluorescence signals below the critical angle are significantly lower than the detection sensitivity and only above the critical angle signals from the bulk are observed. In the presence of a monolayer that provides surface charges, strong fluorescence signals below the critical angle are observed. Ion density accumulated at the interface are determined from the fluorescence. The fluorescent spectra collected as a function of incident x-ray energy near the L_{III} edge yield the extended absorption spectra from the ions, and are compared to recent independent results. The fluorescence data from divalent Ba^{2+} with and without monolayer are also presented.

© 2009 American Institute of Physics

X-ray Fluorescence

- Emission of x-ray from excited elements
 - Absorption removes electron
 - Fluorescence involves inter electron transfers
- x-ray can either be absorbed by the atom or scattered
 - x-ray absorbed by the atom by transferring all of its energy to an innermost electron is photoelectric effect
 - if primary x-ray has sufficient energy electrons are ejected from inner shells, creating vacancies
 - electrons from outer shells are transferred to the inner shells resulting in characteristic x-ray
 - energy is the difference between the two binding energies of the corresponding shells
 - each element produces x-rays at a unique set of energies

X-ray Fluorescence



Introduction

- determination of fluorescence spectra from monovalent ions Cs^+ and divalent ions Ba^{2+}
- the energy dependence of the dispersion corrections of Cs^+ , $f'(E)$ and $f''(E)$, near a resonance

PHYSICAL REVIEW E 72, 060501(R) (2005)

Monovalent counterion distributions at highly charged water interfaces: Proton-transfer and Poisson-Boltzmann theory

Wei Bu, David Vaknin, and Alex Travesset

Ames Laboratory, and Department of Physics and Astronomy, Iowa State University, Ames, Iowa 50011, USA

(Received 1 June 2005; published 1 December 2005)

Experimental setup and methods

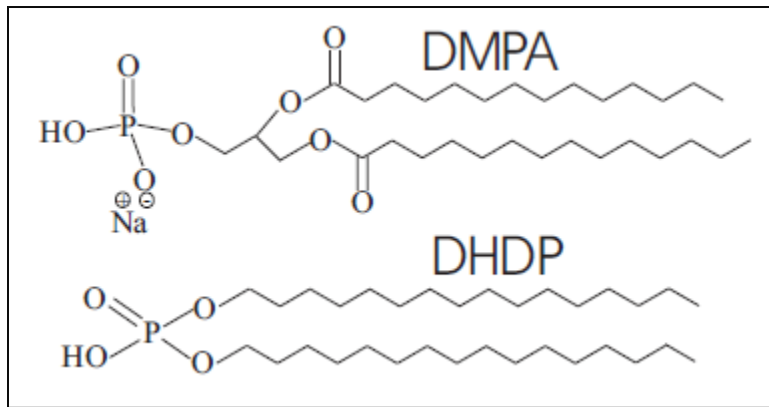


Fig 1. DMPA and DHDP molecules used to form the Langmuir monolayers.

- To form well-controlled interfacial charges, monolayers of DMPA and DHDP were spread at the solution/gas interfaces. [15,16,17]

- ✓ DMPA - dimyristoyl phosphatidic
- ✓ DHDP - dihexadecyl hydrogen phosphate

Catalog No. D2031) were spread from 5.1 mg/100 mL methanol solutions at the air/water interface in a thermostated Langmuir trough [17]. DHDP was chosen for this study, since it forms a simple in-plane structure at high enough surface pressures [18] and its hydrogen-phosphate head group ($R\text{-PO}_4\text{H}$) has a $pK_a=2.1$, presumably guaranteeing almost complete dissociation $[\text{PO}_4^-]/[R\text{-PO}_4\text{H}] \approx 0.99999$, with one electron charge per molecule ($\sigma_0 \approx 0.4 \text{ C/m}^2$).

X-ray reflectivity (XR) and grazing incident x-ray diffraction (GIXD) of monolayers at air/water interfaces were conducted with a Bruker D8 Advance X-ray Diffractometer.

with a 2θ range of 0° to 20° .

The reflectivity is calculated using a model of the discretized density profile, Eq. (1).

Surface pressure versus molecular area of DHDP at various CsI salt concentrations (Fig. 1) were used to control surface-charge density, to identify conditions under which $(\sigma_0=1/A)$ is independent of n_b . For DHDP, two distinct slopes associated with nontilted acyl-chains with respect to the surface were identified by GIXD and rod-scans. In this study, we focus on the parallel

Experimental setup and methods

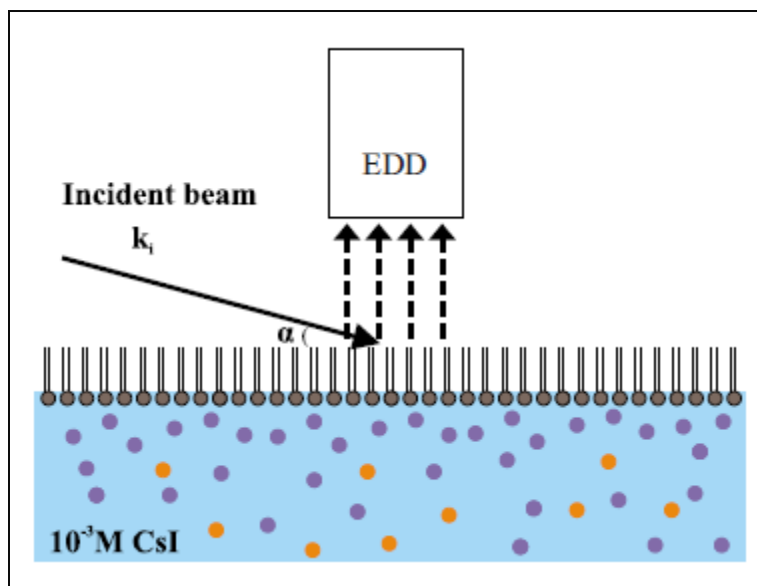


Fig 2. Illustration of the fluorescence experiment setup. The monolayer is spread in an encapsulated Langmuir trough purged with water-saturated helium. The Vortex-EX[®] multicathode x-ray detector window (50 mm² effective detector area) is placed at a distance ~ 2 cm from the surface. The fluorescent beam goes through a thin Kapton window that seals the trough.

- the Ames Laboratory Liquid Surface Diffractometer at the Advanced Photon Source, beamline 6ID-B [18]
- EDD - an energy-dispersive detector

- Si double crystal monochromator
- second monochromator (γ -cut quartz single-crystal d-spacing 4.256 01 Å)
- energy resolution ~ 0.85 eV in the vicinity of the Cs⁺ L_{III} resonances of the ions (~ 5 keV)
- multicathode x-ray detector, used as an EDD
- Kapton window located ~ 2 cm above the liquid surface

Surface ion enrichment

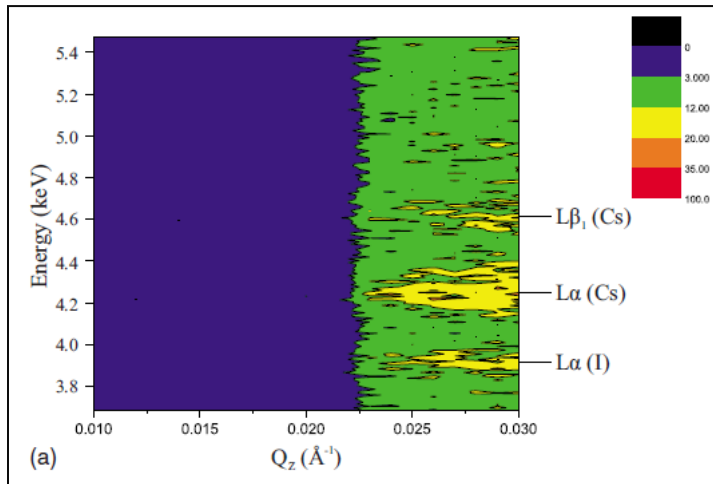


Fig 3. Contour plots of fluorescence intensity for $10^{-3}M$ CsI without (a) and with monolayer DHDP (b). Emission lines are labeled on the right side. Incident x-ray beam energy is 8 keV.

- $Q_z < Q_c$: no significant fluorescence intensity is observed
 - for this concentration the signal from the is significantly lower than the sensitivity of the detector
- $Q_z > Q_c$: the x-ray beam penetrates much deeper ($1-2 \mu m$)
 - this concentration is sufficient to generate fluorescence signals

Surface ion enrichment

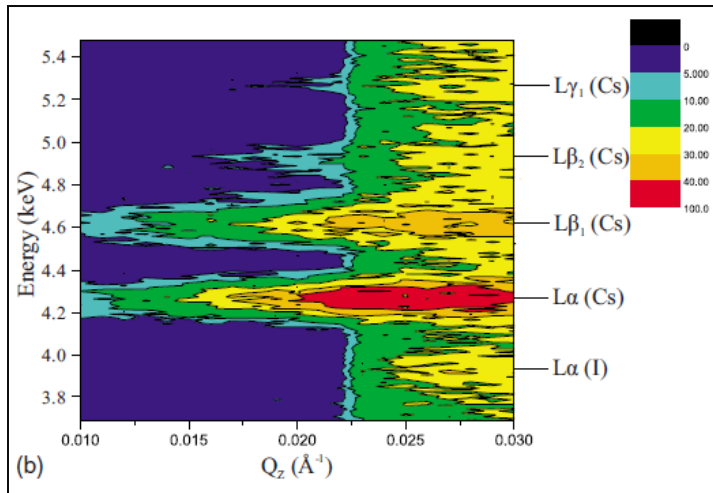
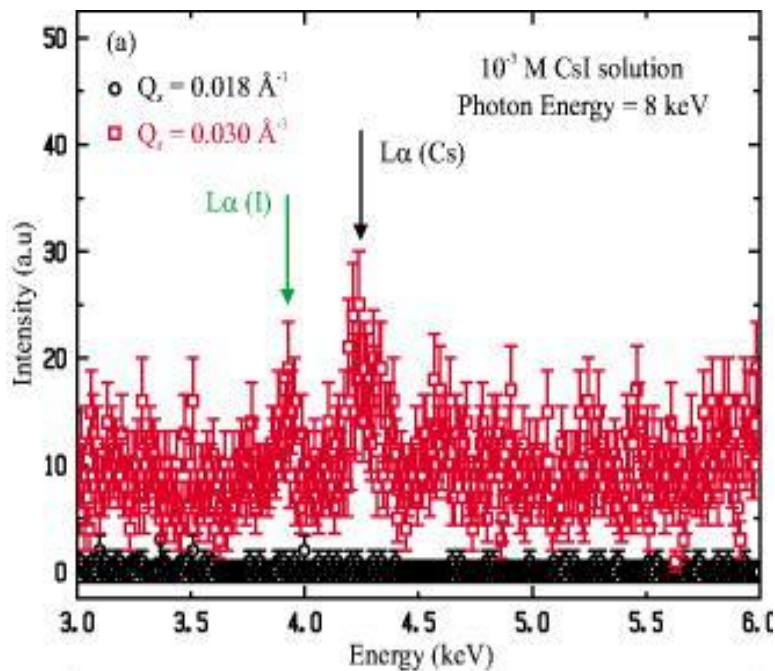


Fig 3. Contour plots of fluorescence intensity for $10^{-3}M$ CsI without (a) and with monolayer DHDP (b). Emission lines are labeled on the right side. Incident x-ray beam energy is 8 keV.

- from that of the bare surface below the critical angle showing emission lines from Cs⁺
- the emission lines include a few weaker ones ($L\beta_2$ and $L\gamma_1$)
 - this is qualitative evidence that Cs⁺ exclusively adsorb at the negatively charged surface
- no emission lines from I⁻, including $L\alpha$, are observed below the critical angle
 - this implies that within the uncertainty in the measurement (about 0.1 ions/DHDP molecule) there is no enrichment of I⁻ at the interface

Surface ion enrichment



- below the critical angle ($Q_z = 0.018 \text{ \AA}^{-1}$)
- above the critical angle ($Q_z = 0.030 \text{ \AA}^{-1}$)

Fig 5.(a) Fluorescence intensity vs. emission line energy for 10^{-3} M CsI below and above the critical angle as indicated. (b) Fluorescence intensity vs. emission line energy at $Q_z = 0.018 \text{ \AA}^{-1}$ with and without monolayer at the interface.

Surface ion enrichment

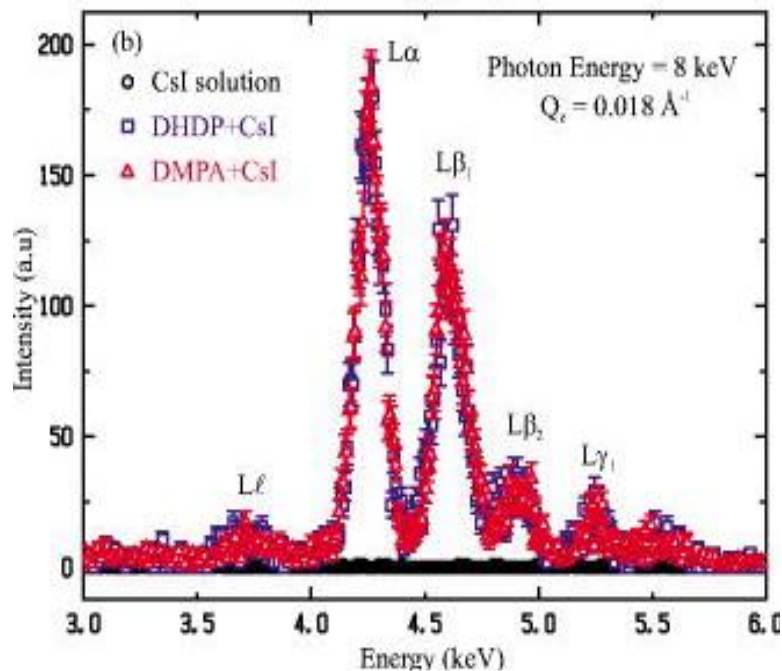


Fig 5.(a) Fluorescence intensity vs. emission line energy for $10^{-3}M$ CsI below and above the critical angle as indicated. (b) Fluorescence intensity vs. emission line energy at $Q_z = 0.018 \text{ \AA}^{-1}$ with and without monolayer at the interface.

- the emission lines from Cs^+ are labeled
- the emission lines of I^- ($L\alpha$, $\sim 3.9 \text{ keV}$) are not detected
- the monolayers have identical fluorescence signals
 - ✓ DHDP and DMPA have similar pK_α (~ 2.1) for the first proton release

Surface ion enrichment

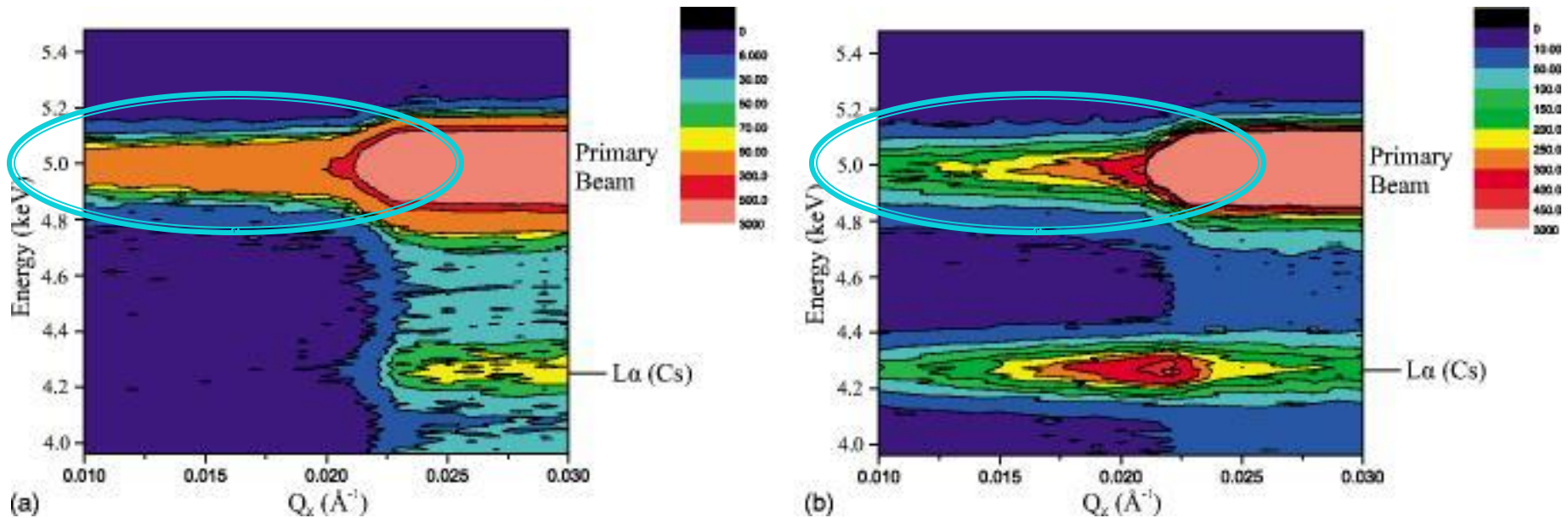


Fig 6. Contour plots of fluorescence intensity for $10^{-3}M$ CsI without (a) and with monolayer DHDP (b). Incident x-ray beam energy is 5.015 keV.

- Contour plots of fluorescence intensity for $10^{-3}M$ CsI with and without the monolayer DHDP with incident x-ray beam energy at the Cs L_{III} resonance
- The strong intensity ridge at approximately 5 keV is due to scattering of the incident beam

Surface ion enrichment

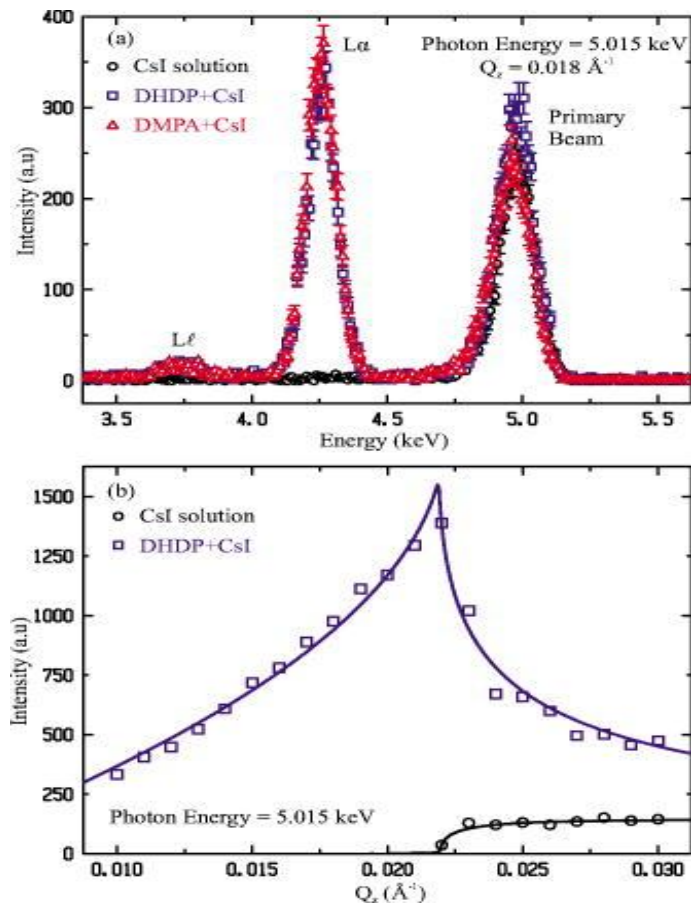


Fig 7.(a) Fluorescence intensity vs. emission line energy at $Q_z = 0.018 \text{ \AA}^{-1}$ with and without monolayer materials (E -cuts from Fig. 6).

(b) Fluorescence intensity of $\text{Cs}^+ L\alpha$ emission line vs. Q_z with and without DHDP (Q_z -cuts Fig. 6).

- Because the incident beam energy is near the $\text{Cs}^+ L_{III}$ resonance, only emission lines from L_{III} ($L\beta, L\alpha,$) are observed
- Without the monolayer, the fluorescence signal is observed only above the critical angle
 - ✓ The intensity slightly increases with Q_z since the penetration depth becomes longer with Q_z [6]
- With the monolayer, fluorescence intensity below the critical angle, due to surface enrichment of Cs^+ at the surface, is observed
 - ✓ This intensity reaches a maximum value at the critical angle due to the multiple scattering [18,22,23]

Surface ion enrichment

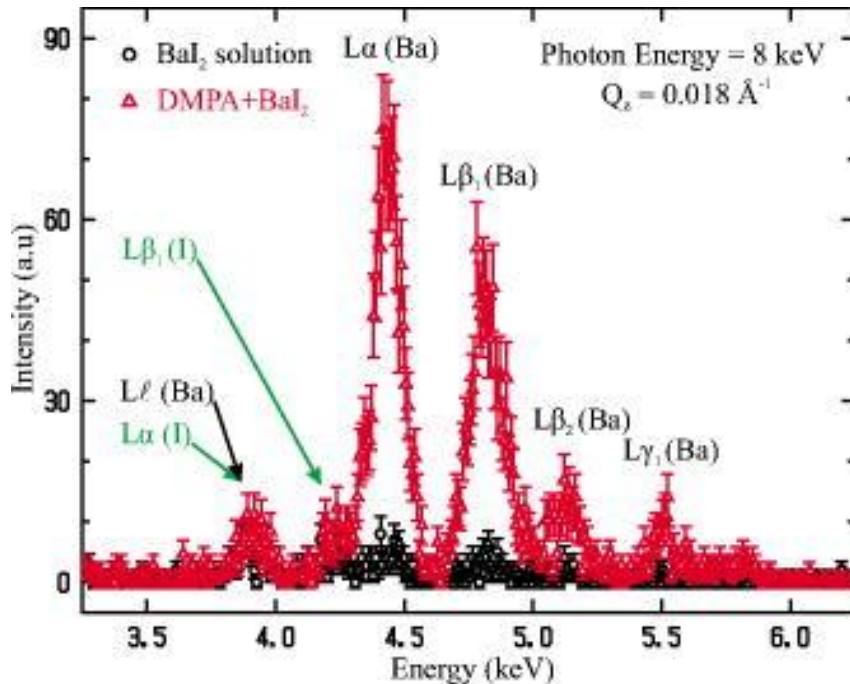


Fig 8. Fluorescence intensity vs. emission line energy for $10^{-2}M$ BaI_2 with and without DMPA at $Q_z = 0.018 \text{ \AA}^{-1}$. Emission lines from both Ba^{2+} and I^- are labeled.

- the emission lines from both Ba^{2+} and I^- are observed below the critical angle for the bare surface solution without the monolayer
- the presence of DMPA charges at the interface enhance the Ba emission lines, with no detectable change in the intensities of the I^- emission lines

Evaluating interfacial ion concentration

- The intensity of the x-ray beam

$$I(z) = I_0 e^{-z/D(\alpha)}$$

where I_0 is the incident beam intensity and $D(\alpha)$ is the penetration depth, which is a function of the incident beam angle (α) and x-ray energy

- The surface scattering is given by

$$I_s = CI_0 AN_{\text{ion}}/A_{\text{lipid}}, \quad (1)$$

and the bulk scattering is

$$I_b = CI_0 A \rho_{\text{bulk}} \int_0^{\infty} e^{-zD(\alpha)} dz = CI_0 A \rho_{\text{bulk}} D(\alpha), \quad (2)$$

where A is the detector area, N_{ion} is the number of ions per lipid, A_{lipid} is the lipid area, and ρ_{bulk} is the ion bulk concentration

- Using Eqs.(1, 2), one can get the number of ions per lipid at the surface using the following relation:

$$N_{\text{ion}} = \frac{I_s(\alpha)}{I_b(\alpha)} A_{\text{lipid}} D(\alpha) \rho_{\text{bulk}}. \quad (3)$$

- The absorption of emitted photons as they traverse to the EDD is negligible since their path in the sample is shorter than that of the incident beam by a factor of at least 100.

Evaluating interfacial ion concentration

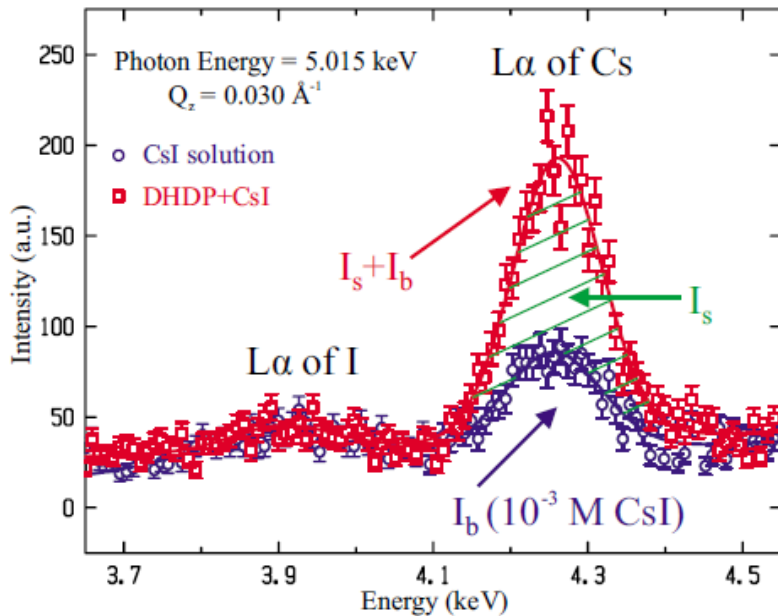


Fig 9. Fluorescence data above the critical angle ($Q_z = 0.030 \text{ \AA}^{-1}$) for $10^{-3}M$ CsI with (I_s+I_b) and without DHDP (I_b). The shaded area represents I_s of Cs^+ $L\alpha$ emission line. X-ray energy is 5.015 keV.

- Spreading monolayer enriches the surface with Cs^+ ions and enhances the $L\alpha$ emission line, but does not change the intensity of I^- $L\alpha$ emission line
- Some of the emission lines from different ions overlap due to the poor resolution of the EDD (150–200 eV)
- The number of ions can be obtained by evaluating I_s and I_b at any Q_z above the critical angle (eq.3)

Evaluating the fine structure $f''(E)$

- The intensity of the emission line is proportional to the absorption of the ion, which is strongly dependent on the photon energy near an absorption edge, and also the immediate environment of the ion.
- By varying the incident beam energy at a fixed Q_z , was obtain the energy dependence of the absorption correction, namely, $f''(E)$ up to a scale factor.

Evaluating the fine structure $f''(E)$

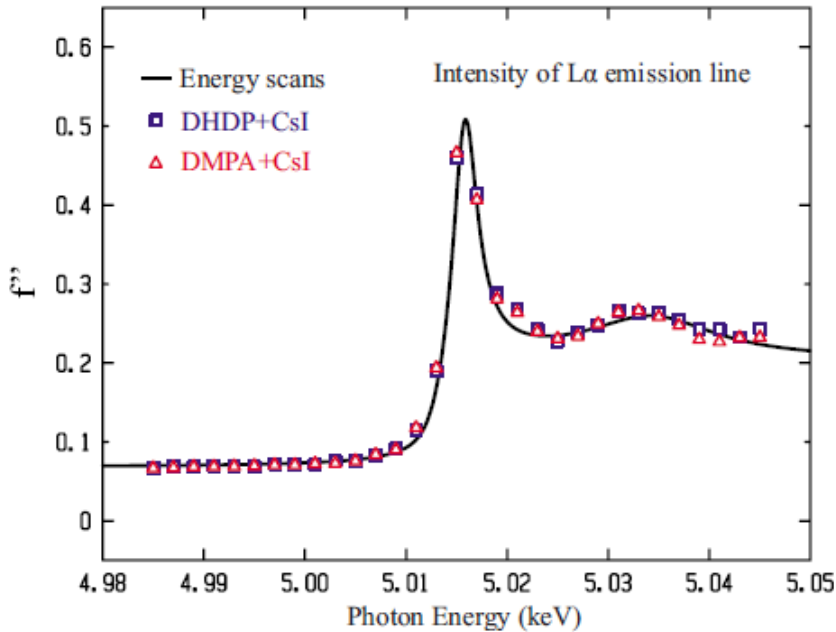
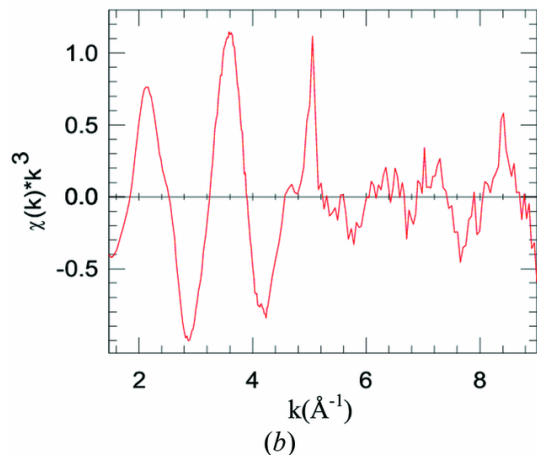
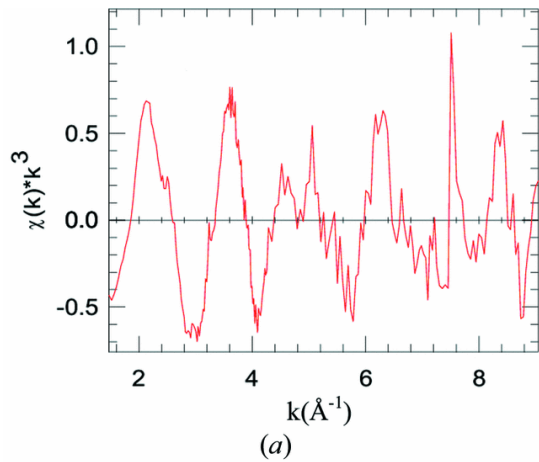


Fig 10. Fluorescence intensity of the Cs^+ $L\alpha$ emission line from $10^{-3}M$ CsI with the monolayers (DHDP and DMPA) at $Q_z = 0.018 \text{ \AA}^{-1}$. The intensity is scaled to the $f''(E)$ far away from the Cs^+ L_{III} resonance ($\pm 30 \text{ eV}$). The solid line is $f''(E)$ obtained by fixed- Q_z energy scans.

- In the vicinity of the resonance, $f''(E)$ of the emitting ion can be influenced by the local environment
- The fluorescence intensity of the Cs^+ $L\alpha$ emission line can be converted to the specific $f''(E)$ in its interfacial environment

Evaluating the fine structure $f''(E)$



Cs L_3 -edge EXAFS $k_3(k)$ spectra for CsNO_3 . (a) BPC6/NPME. (b) BPC6/OA [13]
J.Synchrotron Radiat. **12**, 374 (2005)

- the reported measurement of $f''(E)$ in bulk aqueous environment [13] is slightly different than the here for the Cs^+ L_{III} edge
- differences are from the fact that the ions in this study reside at the interface with a slightly different environment than that in bulk solution

Summary

- The fluorescence technique below the critical angle provides a quick and reliable determination of the presence of ions by identifying the characteristic emission lines of each element that fluoresce
- Calculation of the number density of Cs⁺ ions at the surface by measuring the fluorescence signals with and without the monolayer above the critical angle
- The fine structure of the absorption $f''(E)$ obtained from fluorescence signals measured as a function of photon energy near an absorption edge

Detailed procedures of sample preparations

- CsI solutions in ultrapure water, taking advantage of the L₃ resonance of Cs ions at 5.012 keV in anomalous reflectivity measurements
- monolayers of DHDP were spread from 3:1 chloroform/methanol solutions at the air-water interface in a thermostated Langmuir trough
 - DHDP forms a simple in-plane structure at high enough surface pressures and its hydrogen-phosphate headgroup has guaranteeing almost complete dissociation with one electron-charge per molecule
- monolayers of DHDP were prepared in a thermostatic, solid Teflon Langmuir trough and kept under water-saturated helium environment